

## A Cost-effective Determination of Pressure- and Temperature-Dependent Viscosity of Polymers by Linking Conventional Viscosity Data to PVT Data

Felix Hanselle<sup>1</sup>, Dennis Kleinschmidt<sup>1</sup> and Florian Brüning<sup>1</sup>

<sup>1</sup>Paderborn University, 33098 Paderborn, Germany

### ABSTRACT

The viscosity of polymer melts is dependent on various factors such as shear rate, temperature, pressure and molecular structure. High-pressure capillary rheometry (HPCR) can be used to determine viscosity as a function of shear rate and temperature in the shear rate range relevant for injection molding and extrusion processing. Conventional HPCR measurements cannot determine the pressure dependence of viscosity so that it is typically neglected. Particularly at high pressures and low shear rates, the viscosity is therefore underestimated. However, it is possible to determine the pressure dependency using a counter pressure chamber or actively controlled counter pressure viscometer. Nevertheless, these devices are rarely available, and the measuring effort is high compared to conventional measurements. In order to be able to represent the pressure-dependent material behavior and thus improve the accuracy of process simulations in a cost-effective way, the aim of this paper is to use the free volume approach via the coupled equations of state according to Simha and Somcynsky<sup>1</sup> to link the temperature and pressure dependence of the melt density to the viscosity. The model was extended according to Utracki and Sedlacek<sup>2-4</sup> and applied to true viscosity data at constant shear stresses in the process relevant apparent shear rate range from 1 to 5000 1/s. The necessary viscosity data for the investigated PP and PC at different temperatures in the typical processing range were determined using a conventional HPCR, and a pvT measuring device was used to determine the melt density. The hole fraction as a measure for the free volume is calculated at each shear stress through the coupled equations of state and linked to the true viscosity through error square minimization at the mean pressure in the capillary. This allows for the recalculation of an isobaric viscosity curve at different pressure and temperature levels. For validation of the model viscosities were also measured at various pressure levels using a counter pressure chamber to determine an experimental pressure coefficient. The model results for the investigated materials show a high agreement with the experimentally determined pressure coefficients.

## INTRODUCTION

During plastics processing, such as injection molding and extrusion, the plastic melt is subject to high temperatures, pressures and shear rates. These conditions have a significant effect on the viscosity of the melt, which must be considered when simulating such processes. While the effect of shear rate and temperature has been investigated in many studies and both measurement and consideration in simulation programs are state of the art, the pressure dependence of viscosity is often neglected because of the considerable effort involved in measurement. However, as early as 1957, Maxwell and Jung<sup>5</sup> found that the viscosity of polymers can increase by one or two orders of magnitude when the pressure rises from atmospheric pressure to more than 100 MPa.

The pressure dependence of the viscosity is usually described using the Barus<sup>6</sup> approach as follows:

$$a_p = e^{\beta(p-p_0)} \quad (1)$$

Where  $a_p$  is the pressure shift factor, comparable to the temperature shift factor,  $p$  is the mean pressure in the melt,  $p_0$  is the reference pressure and  $\beta$  is the pressure coefficient. The pressure coefficient for polymer melts ranges from  $10^{-9}$  to  $10^{-8}$  Pa<sup>-1</sup> and varies for different polymers depending on the molecular structure<sup>7-12</sup>. With bulkier side chains, the free volume between the molecular chains is larger, so the free volume decreases with increasing pressure and molecular interactions become stronger<sup>8,9</sup>. This increases intermolecular friction and viscosity<sup>11</sup>.

Furthermore, the same polymer has been shown to exhibit variations in the pressure coefficient. With regards to the shear rate, the coefficient has been observed to both increase and decrease, as well as remain independent<sup>13-16</sup>. Similar observations have been made regarding the temperature dependence of the pressure coefficient<sup>7,13-15,17,18</sup>. These conflicting results highlight the challenges associated with measuring pressure-dependent viscosity data.

Methods for measuring pressure-dependent viscosity include those based on drag flow and pressure driven flow. Koran and Dealy<sup>14</sup> developed a pressurized shear rheometer that allows measurements up to hydrostatic pressures of 70 MPa. However, the achievable shear rate range is typical for a shear rheometer and is with under 500 1/s below the process-relevant range for injection molding.

Capillary rheometers are commonly used to obtain much higher shear rates in the process-relevant range. On the basis of non-linearities in the pressure curve the pressure coefficient can be determined using either a slit capillary<sup>19</sup> or round-hole capillary<sup>20</sup>. Overall, this method is rather inaccurate and only suitable for highly pressure-dependent polymers<sup>9</sup>.

Other methods for determining pressure-dependent data include modified capillary rheometers. In a modified HPCR with a double piston, the melt is pressed through the capillary by one piston, while the other piston actively controls and maintains pressure in the capillary at a constant level<sup>21</sup>. This method is not widely used due to its complexity and high cost.

This study employs a conventional HPCR with a counter pressure chamber extension (CPC) to enable viscosity measurements to be run at elevated pressure levels. **Fig. 1** schematically illustrates the restriction of counter pressure behind the capillary by a throttle. The pressure sensors upstream and downstream of the capillary enable the measurement of viscosity at different pressures by considering the pressure difference and necessary corrections. This set-up has been used in several studies, including those by Laun<sup>22</sup>, Sedlacek et al.<sup>13</sup>, Hausnerova et al.<sup>23</sup>, Cardinaels et al.<sup>11</sup>, Raha et al.<sup>24</sup>, Couch and Binding<sup>7</sup>, and Aho and Syrjälä<sup>9</sup>.

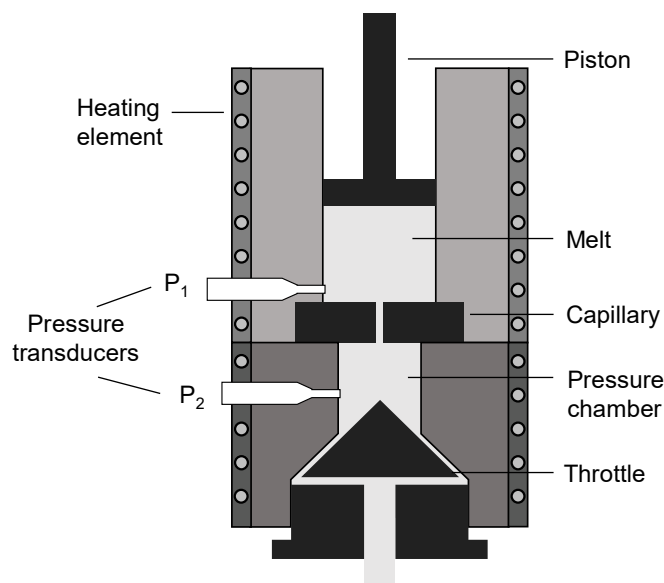


**FIGURE 1:** Schematic of the HPCR with additional counter pressure chamber (schematic based on Yang et al.<sup>25</sup>)

The pressure dependence of viscosity can be determined through one of the mentioned direct methods, but it requires significant effort. Therefore, an indirect method based on one pVT measurement and several conventional viscosity measurements is being explored. The goal is to describe viscosity as complete as possible with as few measurements as possible and at low cost. Based on the coupled equations of state according to Simha and Somcynsky<sup>1</sup> (SS EOS) a calculation procedure is applied and the results are compared with measurements from a HPCR counter pressure chamber.

## MATERIALS AND METHODS

### Materials

For the investigations in this study, an amorphous polycarbonate (PC Makrolon 2400, Covestro, MFI = 20 g/10 min (1.2 kg, 300 °C),  $T_g = 152$  °C) was selected as a typical polymer for injection molding and its particularly high pressure sensitivity. The granulate was dried for 3 h at 120 °C in a dry air dryer before the measurements due to its tendency to absorb moisture. The second material tested was a semi-crystalline polypropylene (PP Moplen HP 420 M, LyondellBasell, MFI = 8 g/10 min (230 °C, 2.16 kg),  $T_m = 166$  °C).

The peak melt temperature  $T_m$  and glass transition temperature  $T_g$  were measured using the dynamic scanning calorimetry apparatus DSC3 Star System from Mettler Toledo (Columbus, United States of America).

### High-Pressure Capillary Rheometer (HPCR) and counter pressure chamber

Both the conventional viscosity measurements and the measurements with the counter pressure chamber were carried out on a Rheograph 50 from Göttfert Werkstoff-Prüfmaschinen GmbH (Buchen, Germany). Round-hole capillaries with a diameter of 1 mm and lengths of 30 and 0.2 mm were used as the test geometry. An apparent shear rate range of 1 to 5000 1/s was considered and the measurements were carried out from high to low shear rates in accordance with ISO 11443<sup>26</sup> by setting an apparent shear rate based on the piston speed. The apparent shear rate  $\dot{\gamma}_{ap}$  was calculated using Eq. 2, which is a function of the volume flow rate  $\dot{V}$  and the capillary diameter  $d$ . The static melting time was 10 minutes for all tests.

$$\dot{\gamma}_{ap} = \frac{32 \cdot \dot{V}}{\pi \cdot d^3} \quad (2)$$

Based on the measured pressure drop  $\Delta p$  in the capillary, the diameter  $d$  and the length  $L$  of the capillary, Eq. 3 is used to determine the apparent shear stress  $\tau_{ap}$ .

$$\tau_{ap} = \frac{\Delta p \cdot d}{4 \cdot L} \quad (3)$$

The apparent viscosity can thus be determined as the quotient of shear stress and shear rate under the following assumptions<sup>21</sup>:

- Fully developed, laminar flow
- Newtonian flow
- Measurement is isothermal
- No pressure dependence
- Wall-adhesive melt

The Bagley correction<sup>27</sup> is used to account for the inlet pressure loss  $\Delta p_e$  due to the geometry, as the pressure is measured upstream of the capillary. To achieve this, measurements are conducted with the two capillaries mentioned, and the inlet pressure loss  $\Delta p_e$  is extrapolated linearly. The true shear stress  $\tau_{tr}$  is then calculated according to Eq. 4.

$$\tau_{tr} = \frac{(\Delta p - \Delta p_e) \cdot d}{4 \cdot L} \quad (4)$$

In the second step, the Weissenberg-Rabinowitsch correction<sup>28</sup> is carried out in order to take into account the shear thinning behavior of the melt. For this purpose, the viscosity data are regressed according to a third-degree polynomial (Eq. 5). The constants  $a_0$ ,  $a_1$ ,  $a_2$  and  $a_3$  are fitting parameters for regressing the viscosity data with the third-degree polynomial. Using the regressed curve, the tangent slope  $n$  of the shear stress over the shear rate is determined for each measured value.

$$\eta = 1 \text{ Pas} \cdot e^{(a_0 + a_1 \cdot \ln(\dot{\gamma} \cdot s) + a_2 \cdot \ln^2(\dot{\gamma} \cdot s) + a_3 \cdot \ln^3(\dot{\gamma} \cdot s))} \quad (5)$$

Accordingly, the true shear rate is determined according to Eq. 6.

$$\dot{\gamma}_{tr} = \frac{(3n+1)}{4n} \cdot \dot{\gamma}_{ap} \quad (6)$$

To experimentally determine the influence of pressure on viscosity, measurements were carried out using the heated counter pressure chamber shown in **Fig. 1**, developed by Göttfert Werkstoff-Prüfmaschinen GmbH. The throttle is used to vary the counter pressure in the chamber so that the average pressure level in the capillary also varies. Tests were conducted on PP and PC at three different temperatures, using both a 30 mm and a 0.2 mm long capillary with a diameter of 1 mm. The throttle restriction remained constant by adjusting the opening angle during each series of measurements. Measurements were taken at apparent shear rates ranging from 10 to 5000 1/s. For each temperature, four different opening angles were tested, in addition to a measurement without restriction. The pressure drop across the capillary was recorded. For the subsequent analysis of inlet pressure loss, all measurements were also conducted using the 0.2 mm long capillary to account for the inlet pressure drop equivalent to conventional measurements, and to implement the Bagley correction.

### **pVT-Measurement**

The pVT measurements were carried out using the PVT500 measuring device from Göttfert Werkstoff-Prüfmaschinen GmbH, Buchen, Germany. Data was collected at pressures ranging

from 10 to 60 MPa with isobaric cooling. The temperature range for PP was 250 – 70 °C and for PC was 330 – 100 °C. These results were later utilized to solve the SS EOS.

### Model on basis of free volume

The free volume refers to the volume created by the vacancies and voids between the molecules<sup>29</sup>. This free volume decreases with an increase in pressure or a decrease in temperature, and vice versa. Simha and Somecynsky introduced the hole fraction  $h$  as the free volume within the framework of lattice hole theory<sup>1</sup>. The calculation is performed by fitting the coupled equations of state, see Eqs. 7 and 8, to the pvT data in the melt region.

$$\frac{\tilde{p}\tilde{v}}{\tilde{T}} = \left[1 - 2^{-\frac{1}{6}} \cdot y(y\tilde{v})^{-\frac{1}{3}}\right]^{-1} + \left(\frac{2y}{\tilde{T}}\right) (y\tilde{v})^{-2} [1.011 \cdot (y\tilde{v})^{-2} - 1.2045] \quad (7)$$

$$[1 + y^{-1} \ln(1 - y)] = \left[2^{-\frac{1}{6}} y(y\tilde{v})^{-\frac{1}{3}} - \frac{1}{3}\right] \cdot \left[1 - 2^{-\frac{1}{6}} y(y\tilde{v})^{-\frac{1}{3}}\right]^{-1} + \left(\frac{y}{6\tilde{T}}\right) (y\tilde{v})^{-2} [2.409 - 3.033(y\tilde{v})^{-2}] \quad (8)$$

The scaling parameters  $\tilde{p} = \frac{p}{p^*}$ ,  $\tilde{v} = \frac{v}{v^*}$  and  $\tilde{T} = \frac{T}{T^*}$  describe the molecular properties of the system based on the characteristic parameters  $p^*$ ,  $v^*$  and  $T^*$ . The parameter  $y = 1 - h$  indicates the occupied site fraction.

The SS EOS are further adjusted to the pvT data by data fitting using the analytical approximation of Simha et al.<sup>30</sup> and the extension of Utracki and Simha<sup>31</sup> by Eq. 9 using the coefficients  $a_0 = -0.10346$ ,  $a_1 = 23.8345$ ,  $a_2 = -0.132$ ,  $a_3 = -333.7$ ,  $a_4 = 1032.5$  and  $a_5 = -1329.9$ .

$$\ln \tilde{v} = a_0 + a_1 \cdot \left(\frac{T}{T^*}\right)^3 \cdot \frac{1}{2} + \left(\frac{p}{p^*}\right) \cdot \left[ a_2 + \left(\frac{T}{T^*}\right)^2 \cdot \left( a_3 + a_4 \cdot \left(\frac{p}{p^*}\right) + a_5 \cdot \left(\frac{p}{p^*}\right)^2 \right) \right] \quad (9)$$

Using the characteristic parameters obtained, the fraction  $h$  can be calculated with the analytical description provided by Utracki and Simha<sup>31</sup> in Eq. 10. The coefficients  $h_0 = 1.203$ ,  $h_1 = -1.929$ ,  $h_2 = 10.039$ ,  $h_3 = 0.729$  and  $h_4 = -218.42$  are therefore applied to calculate hole fraction at different pressures and temperatures.

$$h = h_0 + \frac{h_1}{\tilde{v}} + h_2 \cdot \tilde{T}^{\frac{3}{2}} + \frac{h_3}{\tilde{v}^2} + h_4 \cdot \tilde{T}^3 \quad (10)$$

The correlation between hole fraction and viscosity at constant shear stress  $\eta_c$  is determined using the correlation proposed by Utracki<sup>4</sup>, which has been modified by Sedlacek<sup>2</sup>. Sedlacek provided a better correlation by including the corrected hole fraction  $h'$  in addition to the constants  $C_1$  and  $C_2$  and the hole fraction, as shown in Eq. 11.

$$\ln \eta = \ln C_1 + C_2 \cdot \ln \frac{h'}{h} \quad (11)$$

This corrected hole fraction is determined as a function of the constant  $C_3$  using the reduced compressibility factor, which can be expressed as a ratio of the scaling parameters according to Eq. 13. Sedlacek achieved the highest correlation coefficient for Eq. 11 when  $C_3$  was set to a constant value of 0.25. Therefore, this value was also used in this work.

$$h' = 1 - h \cdot C_3 \cdot \tilde{Z} \quad (12)$$

$$\tilde{Z} = \frac{\tilde{p} \cdot \tilde{v}}{\tilde{T}} \quad (13)$$

The corrected viscosity data were regressed with the Carreau model<sup>32</sup> according to Eq. 14 by means of error square minimization since the viscosity data of the conventional measurements for different temperatures are not available at the same shear stresses. In contrast to Sedlacek's procedure, this work does not use viscosity data from multiple measurement runs with an HPCR with CPC extension for the linkage, but rather viscosity curves measured

conventionally with HPCR at two or three test temperatures. At constant shear stresses, the viscosities were recalculated, and the corresponding mean pressure was determined using Eq. 3, assuming a linear pressure curve in the capillary.

$$\eta = \frac{A}{(1+B\cdot\dot{\gamma})^C} \quad (14)$$

The hole fraction and corrected hole fraction were calculated for each shear stress as a function of mean pressure and temperature using Eqs. 10 and 12. The constants  $C_1$  and  $C_2$  were determined for three temperatures at each shear stress through error square minimization as per Eq. 11. **Table 2** displays the parameters for exemplary shear stresses for PP.

In the following step, isobaric viscosity curves can be calculated for the shear stresses calculated using Eq. 11 at various mean pressures and temperatures.

## RESULTS AND DISCUSSION

To assess the accuracy of the model's calculation of pressure-dependent viscosity data based on free volume, its results are compared with direct measurements using HPCR with counter pressure chamber.

### High-Pressure Capillary Rheometer (HPCR) and counter pressure chamber (CPC)

Both the conventional HPCR measurements and the measurements with different restrictions through the capillary of the counter pressure chamber were first Bagley-corrected and evaluated using an Excel tool. **Fig. 2** (right) shows the average pressure in the capillary for five measurements with different restrictions, which varies depending on the shear rate due to the different piston speeds. In this work, the pressure curve in the capillary is assumed to be linear. Therefore, the mean pressure is equal to the arithmetic mean between the corrected pre-capillary pressure and the post-capillary pressure. Studies by Cardinaels<sup>11</sup> have shown that the error resulting from this simplification of the pressure curve is negligible, at less than 7 %.

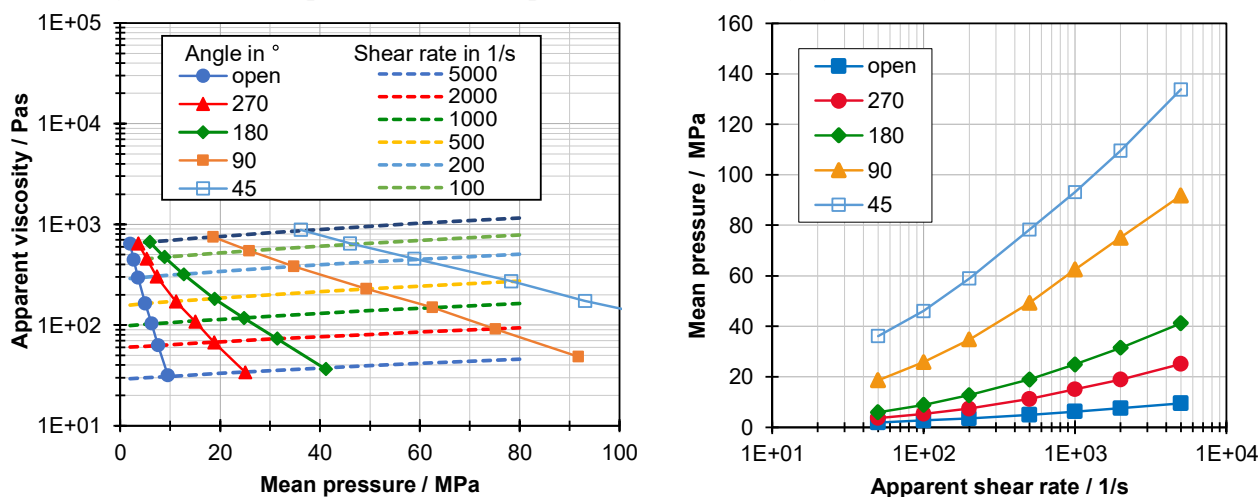


**FIGURE 2:** Measured data and interpolation at fixed apparent shear rates (left) and mean pressure for runs with different throttle positions for PP at 210 °C

As stated earlier, the Bagley-corrected apparent viscosity for constant shear rates is linearly interpolated using the measured data, as depicted in **Fig. 2** (left) for the PP. Based on these interpolations, which are illustrated as dotted lines, the viscosities for pressure levels of 2, 5, 10, 15, 20, 30, 40, 50, 60, and 80 MPa were calculated and corrected in the final step using the Weissenberg-Rabinowitsch correction to account for the non-Newtonian behavior.

The isobaric viscosity curves generated in this way were fitted using the Carreau approach (see Eq. 15 and 1) by means of error square minimization.

$$\eta = \frac{A \cdot a_p}{(1 + B \cdot a_p \cdot \dot{\gamma})^C} \quad (15)$$

**Fig. 3** shows that the Carreau approach accurately describes the isobaric viscosity data. The regression coefficient of determination is greater than 0.9. **Table 3** lists the pressure coefficients of the PP and PC determined using this method. The data for the PC could only be generated at three apparent shear rates with good reproducibility, as shown in **Fig. 3**. The data at lower shear rates were not used for the evaluation due to their low reliability caused by pressure fluctuations during the measurements.

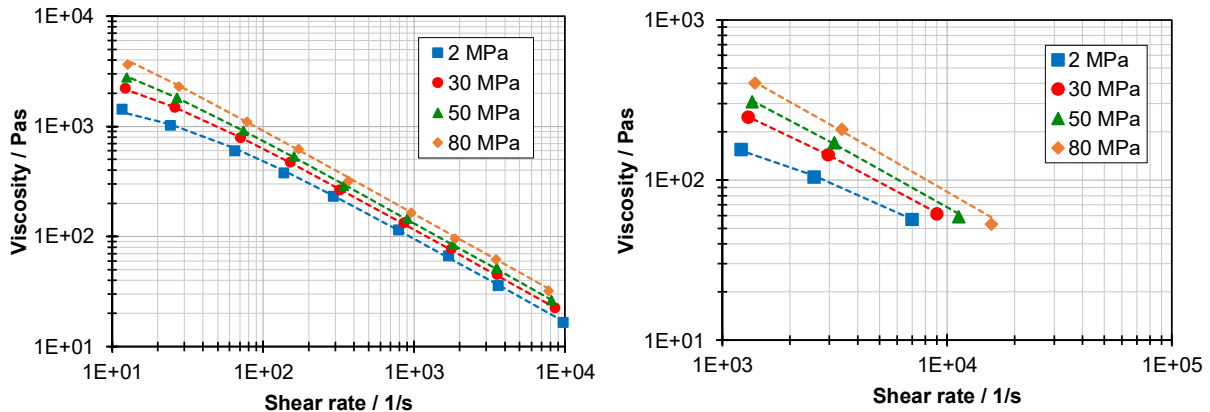


**FIGURE 3:** Viscosity of PP at 190 °C (left) and PC (right) at 300 °C measured with the CPC. Dotted lines represent the regression with Carreau approach

### Results of the model on basis of free volume

The Simha and Somcynsky equations of state were used to fit the pVT data, as described in Eq. 11. Isobaric pVT measurements were conducted on the PP being studied at pressure levels ranging from 10 to 60 MPa and temperatures ranging from 150 to 247 °C. The amorphous PC was analyzed at pressures ranging from 10 to 50 MPa and temperatures ranging from 215 to 315 °C. The resulting characteristic parameters are listed in **Table 1**. The coefficient of determination of 0.9949 (PP) and 0.9863 (PC) for the pressure- and temperature-dependent specific volume, confirms a high degree of agreement. **Fig. 4** illustrates the correlation between the measured specific volume and the calculation according to Eq. 9, shown as a dotted line.

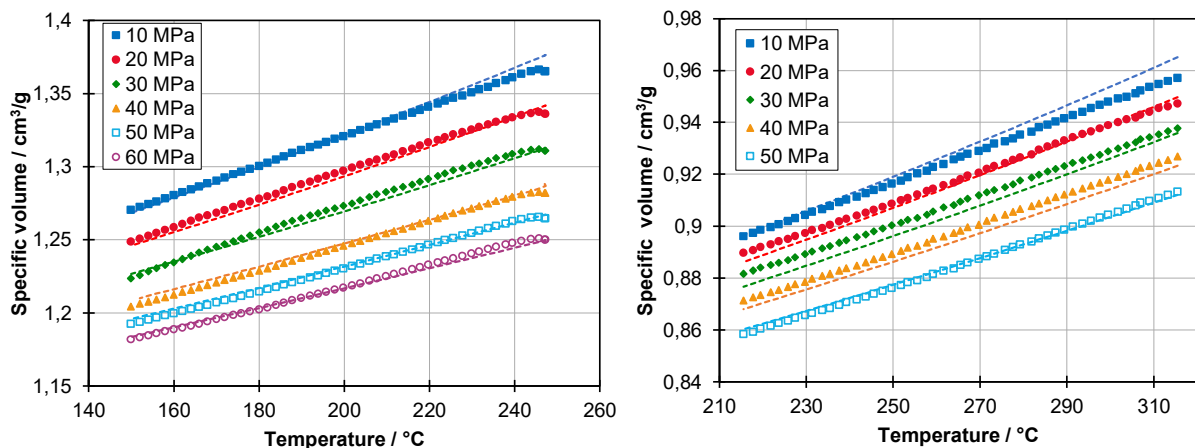


**FIGURE 4:** Isobaric pVT data for PP (left) and PC (right) at various pressures. Dotted lines represent the values calculated through Eq. 9

**TABLE 1:** Characteristic parameters determined through Eq. 9 for PP and PC

Material	T*	p*	v*
-	K	MPa	cm <sup>3</sup> /g
PP Moplen 420 M	28756.1	416.9	1.114
PC Makrolon 2400	10376.1	661.3	0.789

Conventional viscosity data for PP were calculated at 190, 210, and 230 °C for 12 shear stress levels ranging from 5000 to 120,000 Pa. Viscosities for PC were calculated at temperatures of 300, 320, and 340 °C and shear stresses ranging from 10,000 to 600,000 Pa. The hole fraction and corrected hole fraction are then calculated for the individual shear stresses and the flow curves are fitted by Eq. 11. The corresponding constants C<sub>1</sub> and C<sub>2</sub> are listed exemplary in **Table 2** for PP. The parameter C<sub>1</sub>, as defined by Sedlacek to represent viscosity under the assumption of infinite free volume, increases with increasing shear stress, consistent with Sedlacek's findings<sup>2</sup>. Overall, the determined characteristic parameters and constants C<sub>1</sub> and C<sub>2</sub> represent the data with high quality, as shown in **Fig. 5**. The coefficient of determination is greater than 0.999 for both materials.

**TABLE 2:** Determined model constants C<sub>1</sub> and C<sub>2</sub> for PP at different shear stresses

Shear stress [MPa]	Mean pressure [MPa]	Temperature [°C]	Hole fraction [-]	ln(C <sub>1</sub> ) [-]	C <sub>2</sub> [-]
5	0.3	190	0.189	-1.603	5.646
		210	0.204		
		230	0.219		
40	1.8	190	0.186	-3.001	5.619
		210	0.200		
		230	0.215		
70	4.2	190	0.183	-3.854	5.557
		210	0.198		
		230	0.212		
120	7.2	190	0.179	-6.887	6.519
		210	0.193		
		230	0.207		

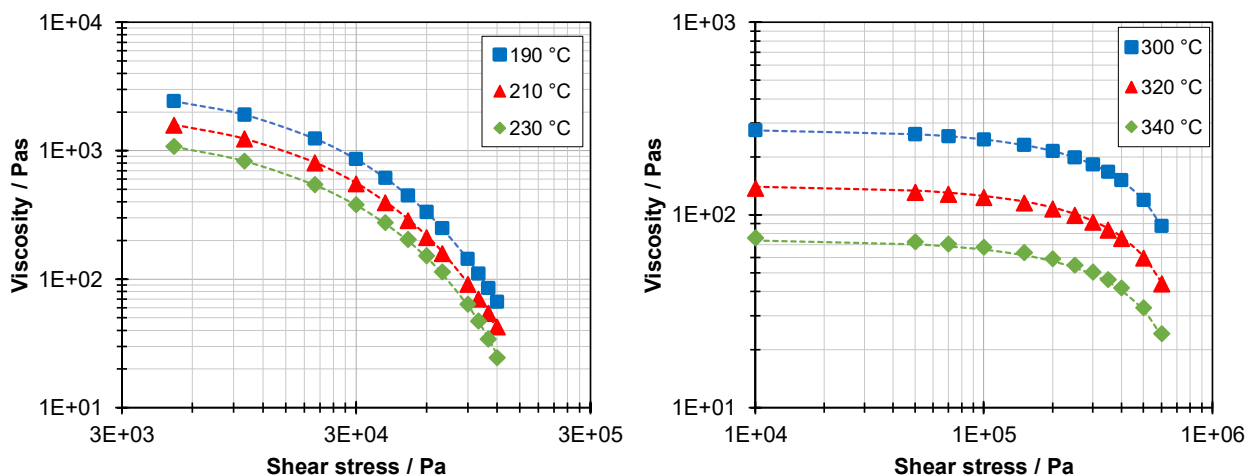


**FIGURE 5:** Input viscosity data and calculated viscosity as dotted lines at constant shear stresses for PP (left) and PC (right)

The linking of pVT data and viscosity allows for the calculation of viscosities at corresponding shear stresses and any mean pressures and temperatures. In this study, viscosities

were calculated at the same pressures and temperatures as those obtained through direct measurement using the CPC. **Fig. 6** displays the model calculations for both the PP and the PC. A high correlation can be observed between the model calculation and the data measured directly using the CPC for the PP. However, the model calculation at constant shear stresses does not depict the high shear rates, especially at high pressures. Therefore, the correlation in this area can only be demonstrated by regressing the data. The evaluation of the model calculation for the PC is limited due to the lack of directly measured data. However, there is solid agreement for the three data points that could be determined by direct measurement when compared to the CPC measurements.

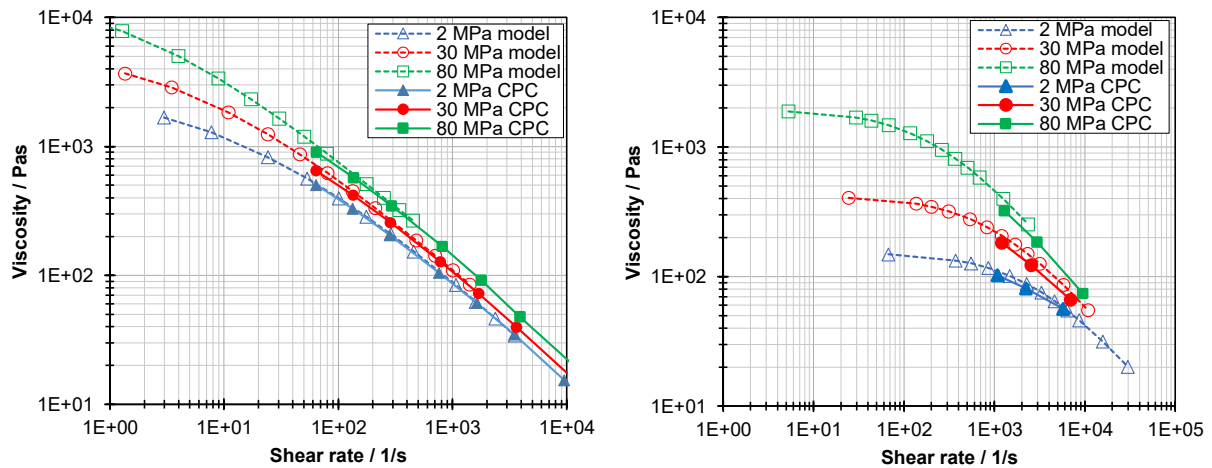


**FIGURE 6:** Viscosity data measured via CPC and data calculated via model for PP (left) at 210 °C and PC (right) at 320 °C for different constant mean pressures

The regression of the model and directly measured data was conducted at various temperatures and mean pressures using the Carreau approach. The pressure shift was determined using Barus approach. The results of this method for determining the pressure coefficient are presented in Table 3, indicating a strong agreement between the two methods. Regarding the relationship between the pressure coefficient and temperature, the CPC measurements showed a decrease in the pressure coefficient with increasing temperature for the PP. The corresponding model calculation determined a pressure coefficient that remains constant over temperature. No trend was observed for the PC examined in the direct CPC measurement but a greater spread, while the pressure coefficient in the model remains constant. Various publications have reported both temperature-invariant<sup>7,16,18,20,33</sup> and decreasing<sup>2,13,15,17</sup> pressure coefficients with temperature. The model results fall within the range of the directly measured results. Further investigations are necessary to confirm whether these results are fluctuations or an actual trend not predicted in the model calculation.

**TABLE 3:** Comparison of pressure coefficient for PP and PC determined through CPC measurements and the model based on pVT data and conventional

	Temperature / °C	Pressure coefficient $\beta$ / 1/GPa	
		Counter pressure chamber	Model
PP	190	25.7	22.3
	210	19.1	22.1
	230	18.8	22.1
PC	300	38.4	31.6
	320	28.8	31.6
	340	32.1	31.8

## CONCLUSION

This work confirms the relationship between the static pressure and temperature dependence of the melt density and the dynamic viscosity for the investigated PP and PC.

Sedlacek<sup>2</sup> determined viscosity data at constant shear stresses and different pressure levels using a HPCR with CPC extension for model application according to Eq. 11 in his publication. Good agreement with experimentally determined data was also demonstrated in this work based on conventionally measured viscosity data at two or three temperatures without the necessity of a CPC extension. The methodology presented in this work offers a significant advantage in that it requires a low measurement effort to determine temperature- and pressure-dependent viscosity data. In these investigations, only four measurement runs of conventional viscosity measurements and one pvT measurement were required for the linkage based on the SS EOS, compared to the 20 or 30 measurement runs required for the comparative measurements with the counter pressure chamber at two or three test temperatures. Additionally, the model can be applied to existing measurement results without further measurements.

The pressure coefficient was determined independently of the shear rate by regression using the Carreau and Barus approach, resulting in a high-quality regression. However, direct measurement using CPC revealed a dependency in the shear rate-dependent calculation of the coefficient. Further investigations are needed to examine this dependency in more detail and validate the methodology for other polymers.

## ACKNOWLEDGEMENTS

The research project (no. 22496 N) described here has been sponsored via the DLR (German Aerospace Center), as part of the program from Industrial Collective Research (IGF), with funds from the German Federal Ministry for Economics and Climate Action (BMWK).

## REFERENCES

1. Simha, R.; Somcynsky, T. On the Statistical Thermodynamics of Spherical and Chain Molecule Fluids. *Macromolecules* **1969**, *2* (4), 342–350. DOI: 10.1021/ma60010a005.
2. Sedlacek, T.; Cermak, R.; Hausnerova, B.; Zatloukal, M.; Boldizar, A.; Saha, P. On PVT and Rheological Measurements of Polymer Melts. *International Polymer Processing* **2005**, *20* (3), 286–295. DOI: 10.3139/217.1890.
3. Utracki, L. A. Pressure dependence of newtonian viscosity. *Polym. Eng. Sci.* **1983**, *23* (8), 446–451. DOI: 10.1002/pen.760230806.
4. Utracki, L. A. A method of computation of the pressure effect on melt viscosity. *Polym. Eng. Sci.* **1985**, *25* (11), 655–668. DOI: 10.1002/pen.760251104.
5. Maxwell, B.; Jung, A. Hydrostatic pressure effect on polymer melt viscosity. *Modern Plastics* **1957**, vol. 35 (no. 3), 174–182.
6. Barus, C. Note on the Dependence of Viscosity on Pressure and Temperature. *Proceedings of the American Academy of Arts and Sciences* **1891**, *27*, 13. DOI: 10.2307/20020462.
7. Couch, M.; Binding, D. High pressure capillary rheometry of polymeric fluids. *Polymer* **2000**, *41* (16), 6323–6334. DOI: 10.1016/S0032-3861(99)00865-4.

8. Goubert, A.; Vermant, J.; Moldenaers, P.; Göttfert, A.; Ernst, B. Comparison of Measurement Techniques for Evaluating the Pressure Dependence of the Viscosity. *Applied Rheology* **2001**, *11* (1), 26–37. DOI: 10.1515/arh-2001-0003.
9. Aho, J.; Syrjälä, S. Measurement of the pressure dependence of viscosity of polymer melts using a back pressure-regulated capillary rheometer. *J. Appl. Polym. Sci.* **2010**, *117* (2), 1076–1084. DOI: 10.1002/app.31754.
10. Fernández, M.; Muñoz, M. E.; Santamaría, A.; Syrjälä, S.; Aho, J. Determining the pressure dependency of the viscosity using PVT data: A practical alternative for thermoplastics. *Polymer Testing* **2009**, *28* (1), 109–113. DOI: 10.1016/j.polymertesting.2008.09.008.
11. Cardinaels, R.; van Puyvelde, P.; Moldenaers, P. Evaluation and comparison of routes to obtain pressure coefficients from high-pressure capillary rheometry data. *Rheol Acta* **2007**, *46* (4), 495–505. DOI: 10.1007/s00397-006-0148-5.
12. Laun, H. M. Pressure dependent viscosity and dissipative heating in capillary rheometry of polymer melts. *Rheol Acta* **2003**, *42* (4), 295–308. DOI: 10.1007/s00397-002-0291-6.
13. Sedlacek, T.; Zatloukal, M.; Filip, P.; Boldizar, A.; Saha, P. On the effect of pressure on the shear and elongational viscosities of polymer melts. *Polym. Eng. Sci.* **2004**, *44* (7), 1328–1337. DOI: 10.1002/pen.20128.
14. Koran, F.; Dealy, J. M. A high pressure sliding plate rheometer for polymer melts. *Journal of Rheology* **1999**, *43* (5), 1279–1290. DOI: 10.1122/1.551046.
15. Kadijk, S. E.; van den Brule, B. H. A. A. On the pressure dependency of the viscosity of molten polymers. *Polym. Eng. Sci.* **1994**, *34* (20), 1535–1546. DOI: 10.1002/pen.760342004.
16. Binding, D. M.; Couch, M. A.; Walters, K. The pressure dependence of the shear and elongational properties of polymer melts. *Journal of Non-Newtonian Fluid Mechanics* **1998**, *79* (2-3), 137–155. DOI: 10.1016/S0377-0257(98)00102-5.
17. Liang, J.-Z. Pressure effect of viscosity for polymer fluids in die flow. *Polymer* **2001**, *42* (8), 3709–3712. DOI: 10.1016/S0032-3861(00)00507-3.
18. Pantani, R.; Sorrentino, A. Pressure Effect on Viscosity for Atactic and Syndiotactic Polystyrene. *Polym. Bull.* **2005**, *54* (4-5), 365–376. DOI: 10.1007/s00289-005-0397-y.
19. Hay, G.; Mackay, M. E.; Awati, K. M.; Park, Y. Pressure and temperature effects in slit rheometry. *Journal of Rheology* **1999**, *43* (5), 1099–1116. DOI: 10.1122/1.551043.
20. Laun, H. M. Polymer melt rheology with a slit die. *Rheol Acta* **1983**, *22* (2), 171–185. DOI: 10.1007/BF01332370.
21. Osswald, T. A.; Rudolph, N. S. *Polymer rheology: Fundamentals and applications*; Hanser Publications: Cincinnati, 2015.
22. Laun, H. M. Capillary rheometry for polymer melts revisited. *Rheol Acta* **2004**, *43* (5), 509–528. DOI: 10.1007/s00397-004-0387-2.
23. Hausnerova, B.; Sedlacek, T.; Slezak, R.; Saha, P. Pressure-dependent viscosity of powder injection moulding compounds. *Rheol Acta* **2006**, *45* (3), 290–296. DOI: 10.1007/s00397-005-0036-4.

24. Raha, S.; Sharma, H.; Senthilmurugan, M.; Bandyopadhyay, S.; Mukhopadhyay, P. Determination of the pressure dependence of polymer melt viscosity using a combination of oscillatory and capillary rheometer. *Polym. Eng. Sci.* **2020**, *60* (3), 517–523. DOI: 10.1002/pen.25307.
25. Liao, Y.; Hu, Y.; Tan, Y.; Ikeda, K.; Okabe, R.; Wu, R.; Ozaki, R.; Xu, Q. Measurement Techniques and Methods for the Pressure Coefficient of Viscosity of Polymer Melts. *Advances in Polymer Technology* **2023**, *2023*, 1–15. DOI: 10.1155/2023/2020247.
26. *ISO 11443 Plastics. Determination of the fluidity of plastics using capillary and slit-die rheometers*; Beuth Verlag GmbH: Berlin, 2021, 83.080.01 (11443:2021).
27. Bagley, E. B. End Corrections in the Capillary Flow of Polyethylene. *Journal of Applied Physics* **1957**, *28* (5), 624–627. DOI: 10.1063/1.1722814.
28. Rabinowitsch, B. Über die Viskosität und Elastizität von Solen. *Zeitschrift für Physikalische Chemie* **1929**, *145A* (1), 1–26. DOI: 10.1515/zpch-1929-14502.
29. Ehrenstein, G. W., Riedel, G., Trawiel, P., Eds. *Praxis der thermischen Analyse von Kunststoffen*; C. Hanser: München, 2004.
30. Simha, R.; Wilson, P. S.; Olabisi, O. Pressure-volume-temperature properties of amorphous polymers: empirical and theoretical predictions. *Kolloid-Z.u.Z.Polymere* **1973**, *251* (6), 402–408. DOI: 10.1007/BF01498686.
31. Utracki, L. A.; Simha, R. Analytical Representation of Solutions to Lattice-Hole Theory. *Macromol. Theory Simul.* **2001**, *10* (1), 17–24. DOI: 10.1002/1521-3919(20010101)10:1<17:AID-MATS17>3.0.CO;2-B.
32. Carreau, P. J. Rheological Equations from Molecular Network Theories. *Transactions of the Society of Rheology* **1972**, *16* (1), 99–127. DOI: 10.1122/1.549276.
33. Sorrentino, A.; Pantani, R. Determination of the effect of pressure on viscosity of an isotactic polypropylene. *Polym. Bull.* **2013**, *70* (7), 2005–2014. DOI: 10.1007/s00289-013-0913-4.